JOURNAL OF MATERIALS SCIENCE 31 (1996) 1569–1573

Effect of titanium substitution on the structure and properties of Fe_3Al-based intermetallic alloys

U. PRAKASH, K. MURALEEDHARAN
Defence Metallurgical Research Laboratory, P.O. Kanchanbagh, Hyderabad 500258, India
R. A. BUCKLEY, H. JONES, P. A. SHENTON
Department of Engineering Materials, University of Sheffield, UK

Substitutions (0–16 at%) of titanium for iron in Fe_3Al-based alloys rapidly solidified by chill-block melt-spinning stabilize the $D0_3$ and B2 ordered structures. Rapid solidification results in total suppression of $D0_3$ order in binary alloys, whereas alloys containing titanium have $D0_3$ structure. $D0_3$ and B2 antiphase domain size, lattice parameter and hardness increase with increasing titanium content of the alloy. The deformation mode changes from single (unit) bcc dislocation in binary alloys to two-fold superdislocation configuration in $D0_3Fe_3Al$–Ti alloys. Mechanical antiphase boundaries are generated by the movement of these imperfect configurations. All the alloys exhibited cleavage tensile failure. The mechanical properties are correlated with the observed structural changes.

1. Introduction

Ordered alloys based on the intermetallic $D0_3Fe_3Al$ are being developed for high-temperature structural applications [1, 2]. Although these alloys can exhibit brittle behaviour at low homologous temperatures, substantial improvement in mechanical properties can be achieved by application of techniques such as rapid solidification processing [1–3]. The ordering temperature (and therefore service temperature) $D0_3Fe_3Al$ alloys may be significantly increased by substitutional additions of elements such as titanium and molybdenum [1, 2, 4]. The present work investigated the structure and mechanical properties of rapidly solidified Fe-27Al (all compositions in at%) alloys with ternary titanium substitutions for iron.

2. Experimental procedure

Fe–27Al alloys containing 0, 6, 12 and 16% Ti were made by melting pure (99.99%) iron and aluminium and an Al-60 wt% Ti master alloy in alumina crucibles in a controlled-atmosphere induction furnace and chill casting into ingots of 25 mm diameter and 200 mm long using a mild steel split mould. From these, small (5–10 g) samples of the alloys were then remelted and rapidly solidified by chill-block melt-spinning in an argon atmosphere using a mild steel substrate. The melt-spinning conditions employed were as follows: ejection pressure 40×10^3 kPa (6 lbf in^{-2}), nozzle diameter 1 mm, nozzle angle 10° to the vertical, and wheel speed 24 $m\,s^{-1}$.

The ribbon samples were mounted, with the side previously in contact with the wheel uppermost, for studies in a Philips 1710 X-ray diffractometer using CoK_α radiation. Lattice parameters were calculated from high-angle reflections (3 1 0 and 2 2 0) using standard extrapolation methods [5]. Microhardness (Knoop) readings were taken along cross-sections of ribbons mounted in bakelite and polished to 0.25 μm grade diamond finish. The ribbon sections were etched using Kellers reagent (1% HF, 1.5% HCl and 1.5% HNO_3 by volume in water) and studied in a Jeol 840 scanning electron microscope (SEM). The ribbons were fractured in tension in an Instron machine. Samples with high (12% or more) titanium contents too brittle to be gripped in the machine were manually broken in tension. The resulting tensile fracture surfaces were observed in the SEM. As-cast as well as as-deformed ribbon samples for transmission electron microscopy (TEM) were prepared in a Fischione electropolishing unit using a 40 V d.c. voltage and 5% perchloric acid in ethanol at −20 °C as electrolyte.

3. Results

SEM revealed ribbon cross-sections typically 30–35 μm across with columnar grains growing from the side previously in contact with the wheel (Fig. 1). X-ray and electron diffraction showed that the $D0_3$ order was totally suppressed in the Fe-27Al ribbon but the ribbons containing titanium exhibited $D0_3$ structure. The average grain size observed in the TEM was 3–5 μm and was not significantly dependent on the composition. The B2 and $D0_3$ antiphase domain (APD) size increased with increasing titanium content of the ribbon (Figs 2a–c and 3a–c). In Fe–27Al–16Ti alloy the B2 domain size was the same as the grain size

0022–2461

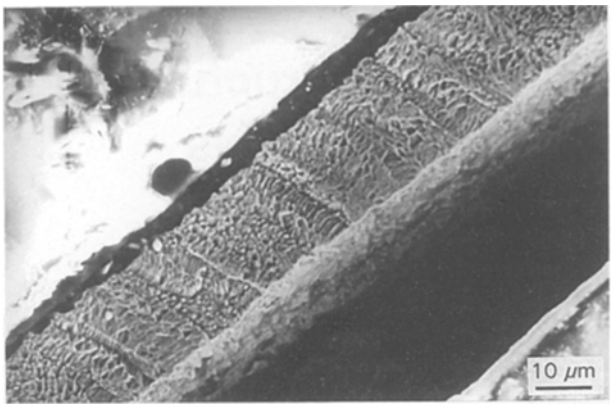

Figure 1 Scanning electron micrograph showing columnar grains in melt-spun Fe–27 Al ribbon.

and no B2 antiphase boundary (APB) networks were observed. Possible dislocation configurations in ordered Fe–Al alloys are shown in Fig. 4. Mechanical B2 APBs (Fig. 2a) were observed in the Fe–27Al ribbons indicating deformation by the unit $a\langle 1\,1\,1\rangle/2$ bcc dislocations (Fig. 4d). Weak beam (Fig. 5a and b) and centred dark-field (Fig. 3a) images showed that there is a transition to deformation by the two-fold imperfect superlattice dislocation configuration (Fig. 4c) in alloys containing titanium which exhibit DO_3 order. The spacing between the dislocations in the configuration decreased with increasing titanium content (Fig. 5a and b). The four-fold dislocation configuration (Fig. 4b) was not observed in any of the ribbons. All the ribbons were found to undergo cleavage failure (Fig. 6). The lattice parameter, as well as hardness of the ribbons, was found to increase significantly with increasing titanium content (Fig. 7a and b).

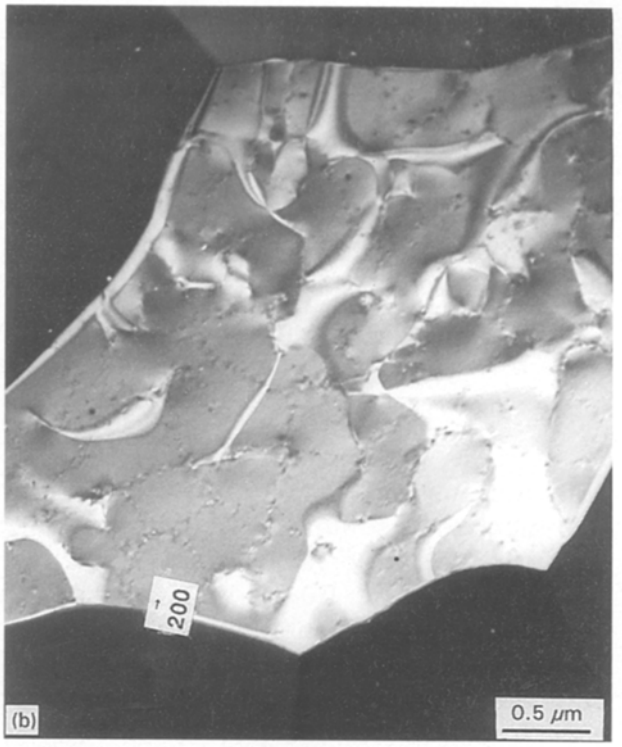

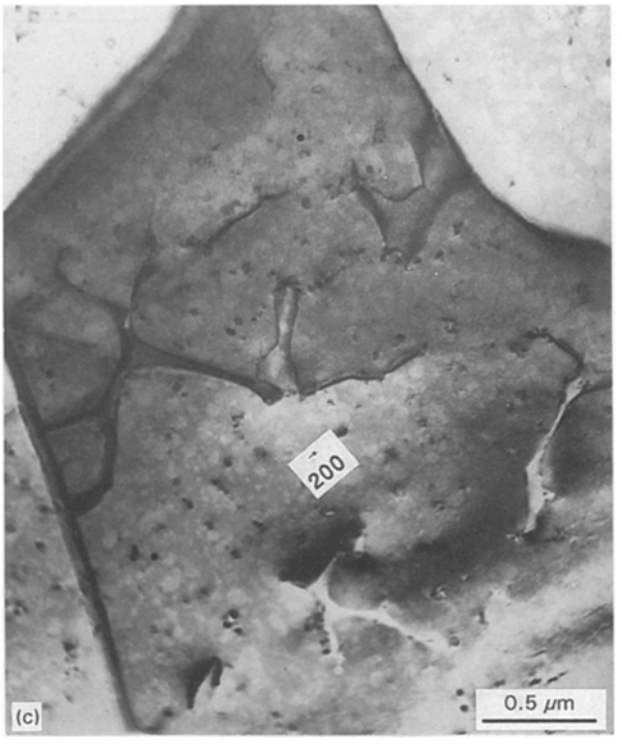

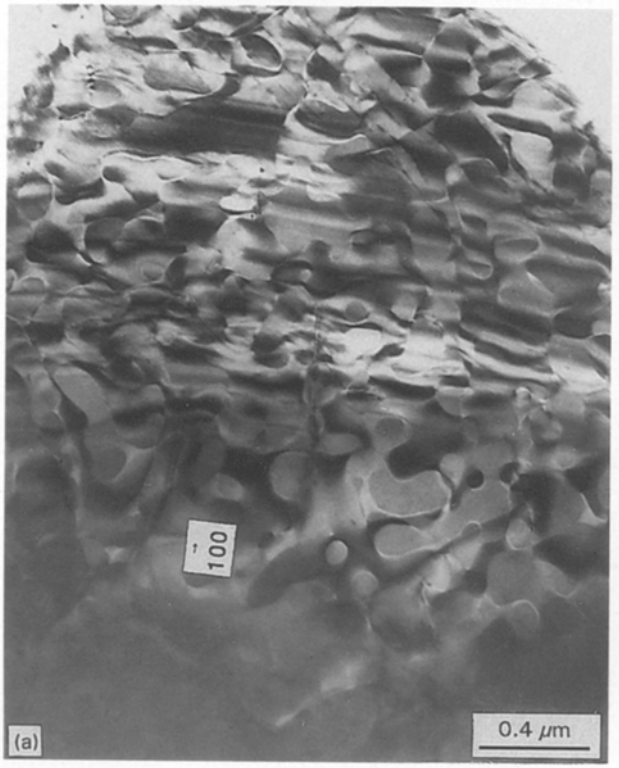

Figure 2 Centred dark-field transmission electron micrographs showing increasing B2 antiphase domain size with increasing titanium content in ribbons with (a) 0%, (b) 6% and (c) 12% Ti. Note the B2 mechanical APBs (a) in the deformed Fe–27Al ribbon created by the unit (bcc) dislocation configuration shown in Fig. 4d.

4. Discussion

The increase in lattice parameter (Fig. 7a) with increasing titanium content may be explained by noting that titanium atoms are larger in size than the iron atoms they replace. For metallic bonding conditions, atomic radii of 0.145 and 0.125 nm have been assigned to titanium and iron respectively [6]. Titanium

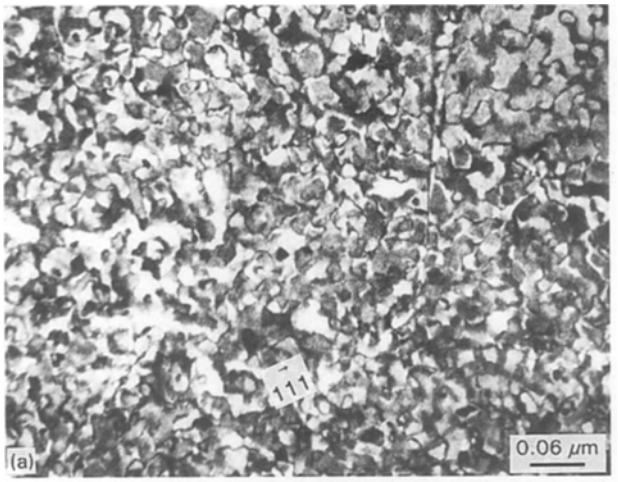

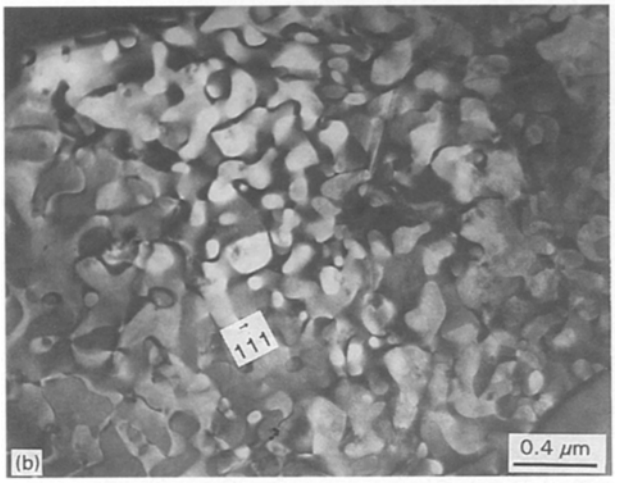

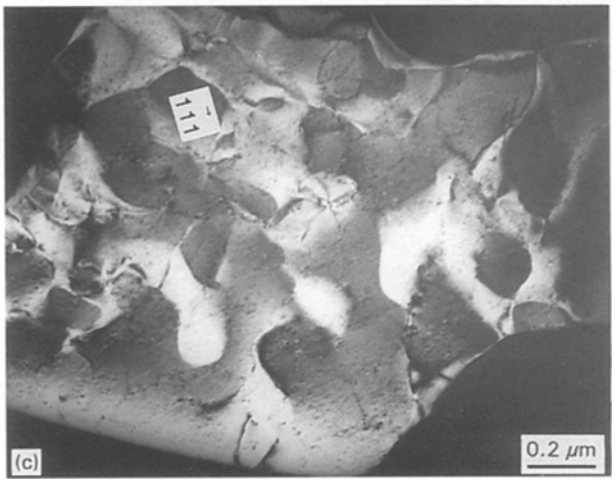

Figure 3 Centred dark-field transmission electron micrographs showing increasing $D0_3$ antiphase domain size with increasing titanium content in ribbons with (a) 6% (b) 12% and (c) 16% Ti. Note the $D0_3$ mechanical APBs in (a) created by the dislocation configuration shown in Fig. 4c.

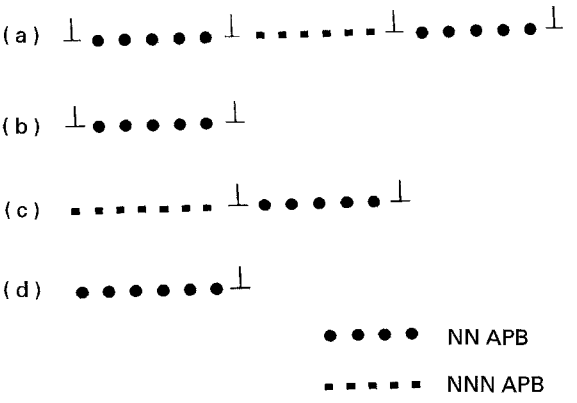

Figure 4 Dislocation configurations in ordered Fe–Al alloys: (a) $D0_3$ dislocation configuration; (b) B2 dislocation configuration; (c) passage of an imperfect dislocation configuration in the $D0_3$ lattice; (d) passage of a unit dislocation in B2 and $D0_3$ lattice. The Burgers vector of the individual dislocations in the configuration shown is $a\langle 1\,1\,1\rangle/2$ or $a''\langle 1\,1\,1\rangle/4$ where a and a'' are the lattice parameters of the B2 and the corresponding $D0_3$ unit cells, respectively. NN APB and NNN APB represent nearest neighbour ($a\langle 1\,1\,1\rangle/2$ or $a''\langle 1\,1\,1\rangle/4$ type) and the next nearest neighbour ($a''\langle 1\,0\,0\rangle/2$ type) antiphase boundaries, respectively.

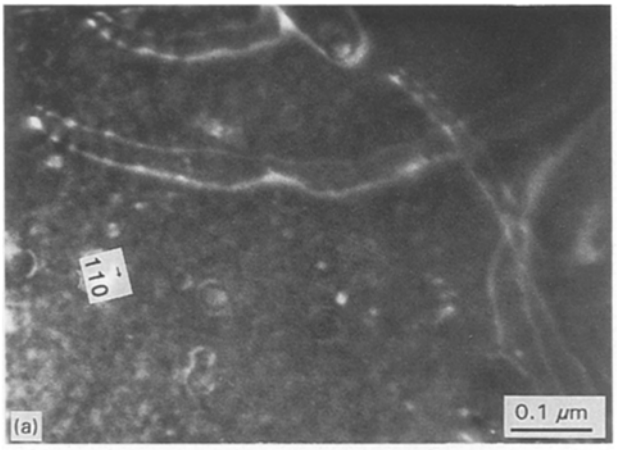

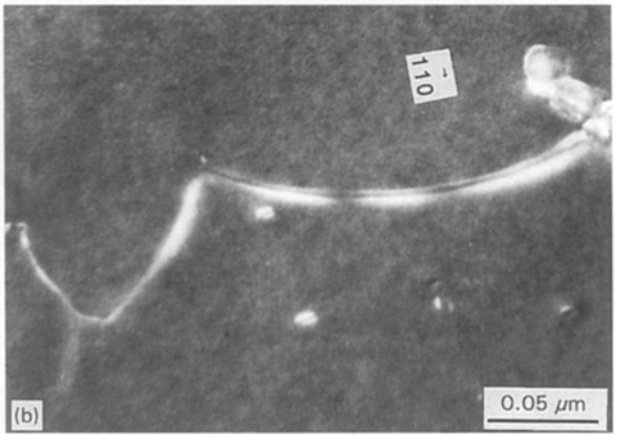

Figure 5 Weak-beam transmission electron micrographs showing superlattice dislocation pairs of the type shown in Fig. 4c in ribbons containing (a) 6% and (b) 12% Ti. Note the decrease in spacing between dislocations constituting the pair with increase in titanium content.

substitutions for iron would, therefore, result in an increased amount of misfit, thus increasing the size of the unit cell. The accompanying increase in hardness (Fig. 7b) may also be largely attributed to the solid-solution strengthening arising out of this misfit.

Titanium substitutions for iron in Fe_3Al-based alloys are known to increase the $D0_3$ ordering temperature [1, 2, 4]. Thus the $D0_3$ order is suppressed in the rapidly solidified binary alloy where the ordering is relatively weak but not in the strongly ordered titanium-containing alloys. The $D0_3$ domains in alloys with high titanium content form at higher temperatures where the diffusion rates and, therefore, the

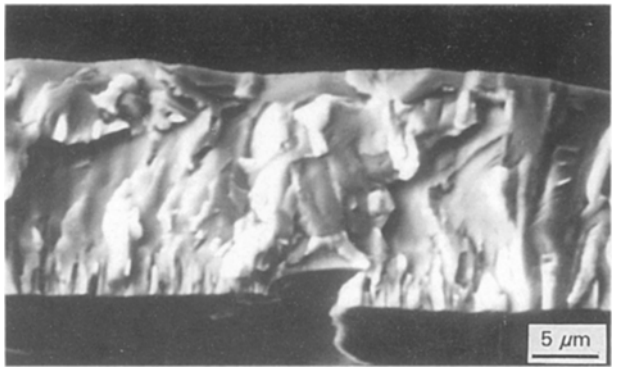

Figure 6 Scanning electron micrograph showing cleavage tensile failure in Fe–27Al–16Ti ribbon.

APB mobilities are higher, allowing the domains to grow to relatively larger sizes before the microstructure is "frozen-in". The increase in DO_3 domain sizes with increasing titanium content may thus be explained. Because the B2 domain size also increases with increasing titanium content it may be argued that titanium substitution for iron also raises the B2 ordering temperature. This is also supported by the change in dislocation configuration from unit dislocation (Fig. 4d) to imperfect superlattice dislocation (Fig. 4c) with increase in titanium content. At higher titanium contents the B2 APB (NN APB) energy is larger, ensuring that the dislocations are in pairs (Fig. 4c). The separation between the unit (b c c) dislocation constituting the pair decreases with increasing titanium content (Fig. 5a and b) and this also may be attributable to the relatively higher B2 APB energy [7]. Although the corresponding DO_3 APB energy also increases, the increase is probably not enough to hold the two outer pairs (Fig. 4a) together. These uncouple, resulting in the imperfect configuration (Fig. 4c) observed in the present work.

It has been argued [8, 9] for the binary Fe–Al alloys, that thermal and/or mechanical APBs contribute to stress homogenization by interacting with dislocations, preventing intergranular failure and resulting instead in cleavage failure at aluminium contents of up to 37%. Likewise, in the Fe_3Al–Ti ribbons, both mechanical and thermal domains are present and the fracture occurs by cleavage. In strongly ordered rapidly solidified binary Fe–Al alloys where B2 APD size equals the grain size, DO_3 domains are not present and, in the absence of significant dislocation–APB interactions, these fail intergranularly [8]. The present work thus shows that it is possible to extend the cleavage failure regime to alloys with high ordering temperatures.

5. Conclusions

1. Substitution of titanium for iron in Fe_3Al results in increase of B2 and DO_3 ordering temperatures.

2. The lattice parameter increases with increasing titanium substitution. The accompanying increase in hardness may largely be attributable to solid-solution strengthening with possible contributions from dislocation–APB interactions.

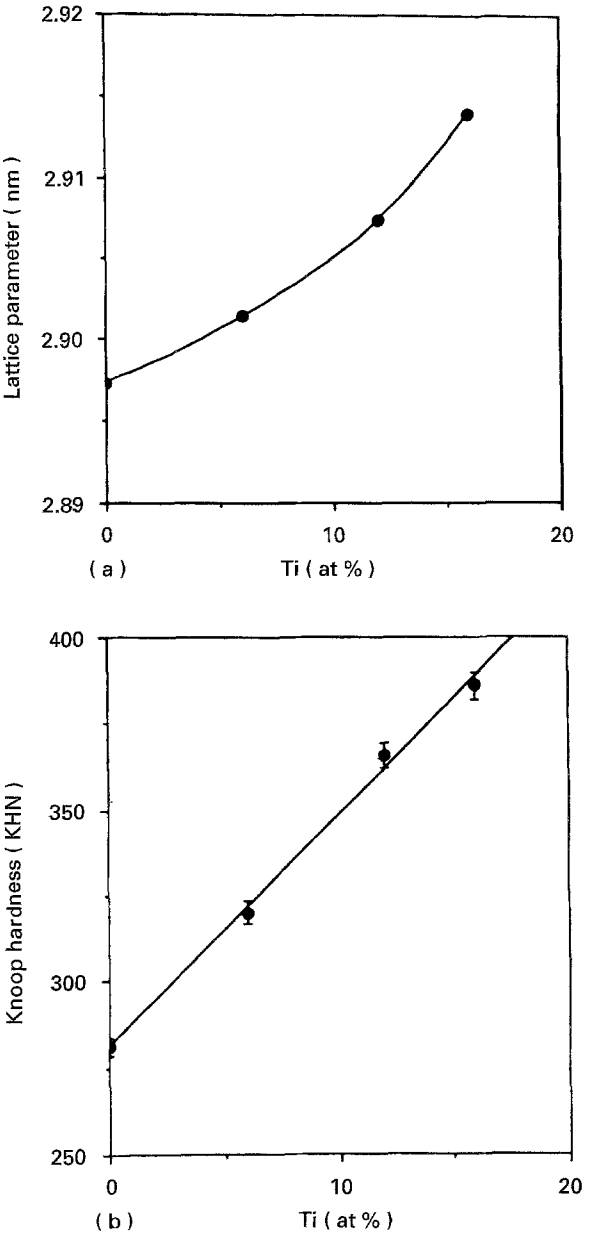

Figure 7 Variation of (a) lattice parameters, and (b) hardness with composition. For the binary B2 ribbon, the equivalent DO_3 lattice parameter is taken.

3. Rapid solidification results in total suppression of DO_3 order in binary Fe–27Al, whereas alloys containing titanium have DO_3 structure. DO_3 and B2 antiphase domain size increase with increasing titanium content.

4. The deformation mode changes from unit (b c c) dislocation in binary alloys to two-fold superdislocation configuration in DO_3Fe_3Al–Ti alloys. Mechanical APBs, generated by movement to these imperfect dislocations, were observed.

5. All the alloys exhibited tensile cleavage failure. This is interpreted in terms of dislocation–APB interactions.

Acknowledgements

U.P. and K.M. thank the Director, DMRL, for provision of laboratory facilities and permission to publish this work. At Sheffield, the work was supported by the

Science and Engineering Research Council (UK). London and Scandinavian Metals Ltd, Rotherham, kindly supplied the Al–Ti master alloy used.

References

1. C. G. MCKAMEY, J. H. DEVAN, P. F. TORTORELLI and V. K. SIKKA, *J. Mater. Res.* **6** (1991) 1779.
2. U. PRAKASH, R. A. BUCKLEY, H. JONES and C. M. SELLARS, *ISIJ Int.* **31** (1991) 1113.
3. C. C. KOCH, *Int. Metall. Rev.* **33** (1987) 201.
4. M. G. MENDIRATTA, S. K. EHLERS and H. A. LIPSITT, *Metall. Trans.* **18A** (1987) 509.
5. B. D. CULLITY, in "Elements of X-ray Diffraction" (Addison Wesley, London, 1978).
6. A. H. COTTRELL, in "An Introduction to Metallurgy" (Arnold, London, 1985) p. 35.
7. M. J. MARCINKOWSKI and N. BROWN, *J. Appl. Phys.* **33** (1962) 537.
8. U. PRAKASH, R. A. BUCKLEY, H. JONES and G. W. GREENWOOD, *Philos. Mag.* **65A** (1992) 1407.
9. *Idem, Philos. Mag. Lett.* **65** (1992) 129.

Received 3 June 1994
and accepted 8 September 1995